Hindawi Publishing Corporation
International Journal of Antennas and Propagation
Volume 2012, Article ID 386846, 7 pages
doi:10.1155/2012/386846

*Research Article*

# Design of High Gain and Broadband Antennas at 60 GHz for Underground Communications Systems

**Yacouba Coulibaly,[1] Mourad Nedil,[1] Larbi Talbi,[2] and Tayeb A. Denidni[3]**

[1] *LRTCS-UQAT, 450 3eme Avenue Local 105, Val-d'Or, QC, Canada J9P1S2*
[2] *UQO, 283 Boulevard Alexandre-Taché Gatineau, QC, Canada J9A 1L8*
[3] *INRS-EMT 800, De La Gauchetière Ouest Bureau 6900, Montréal, QC, Canada H5A 1K6*

Correspondence should be addressed to Mourad Nedil, mourad.nedil@uqat.ca

Received 26 September 2011; Revised 15 January 2012; Accepted 16 January 2012

Academic Editor: Deb Chatterjee



A new broadband and high gain dielectric resonator antenna for millimeter wave is presented. The investigated antenna configuration consists of a periodic square ring frequency selective surfaces on a superstrate, an aperture-coupled scheme feed, an intermediate substrate, and a cylindrical dielectric resonator. This antenna is designed to cover the ISM frequency band at 60 GHz (57 GHz–64 GHz). It was numerically designed using CST microwave Studio simulation software package. Another prototype with a plain dielectric superstrate is also studied for comparison purposes. A bandwidth of 13.56% at the centered frequency of 61.34 GHz and a gain of 11 dB over the entire ISM band have been achieved. A maximum gain of 14.26 dB is obtained at 60 GHz. This is an enhancement of 9 dB compared to a single DRA. HFSS is used to validate our antenna designs. Good agreement between the results of the two softwares is obtained. With these performances, these antennas promise to be useful in the design of future wireless underground communication systems operating in the unlicensed 60 GHz frequency band.

## 1. Introduction

The progress of communication technologies over the last decades has been spectacular in confined areas such as tunnels and underground mines. Underground mines are considered to be dangerous, hazardous, and aggressive environments. Wireless communications are essential for several reasons including safety, security, and productivity [1]. In recent years wireless communication systems have been deployed successfully at millimeter waves band, especially in the 57 GHz–64 GHz range. This frequency band is of great interest due to the massive universal unlicensed spectrum around 60 GHz available for short-range communication systems [2, 3]. The use of this frequency band also exhibits interesting features such as high available bandwidth, high capacity, and the promise of short frequency reuse distances [2]. The disadvantage of millimeter waves is that the absorption of atmosphere is increased significantly beyond about 20 GHz due to the effect of oxygen molecules and water vapor [2]. This oxygen absorption is about 16 db/km at 60 GHz. Another disadvantage is propagation losses, which are about 30 dB higher than at 2 GHz in free space. Therefore, this band is not appropriate for long-range communications, but very suitable for short range including indoor communications and underground communications. High path losses and oxygen absorption can be overcome with high transmit power available by the regulation around 60 GHz and high gain antennas.

Dielectric Resonators Antennas (DRA) might serve as an attractive alternative to planar antennas for ISM communications. They are not affected by narrow bandwidth and they do not have high conduction loss at millimeter wave frequencies or low efficiency due to surface wave excitation, as DRA require no radiating metal patch [4]. The other advantages of DRA include reduced size, linear and circular polarizations, and availability of different radiation patterns by exciting different radiation modes. However, antennas of this type generally offer a gain around 6 dBi. Among commonly used gain improvement approaches are stacking dielectric resonators [5], using surface mounted short horn [6] and combining

a DRA in tandem with an electromagnetic band gap structure [7]. The bandwidth of DRA is also limited to 10% for a single mode operation. The demand of high-rate data transmission in wireless communication systems has contributed to the development of many schemes to increase the bandwidth of DRA [8–10]. Superstrates, such as Frequency Selective Surfaces (FSS), Electromagnetic Band Gap (EBG) metamaterials, and dielectric slabs, are emerging as alternatives to improve the gain of an antenna [11–19]. A Fabry-Perot resonant cavity is formed by the ground plane of the primary antenna and the superstrate. Some examples for the potential application superstrates in the 60 GHz-unlicensed frequency band have been proposed [17–19]. A microstrip patch antenna is combined with three layers of a metamaterial superstrate to achieve a gain of 19 dB [17]. Another patch with a single dielectric superstrate is presented. A measured gain of 14.6 dBi is obtained, which is 9 dB higher than the gain of a single patch antenna [18]. The guidelines to design a 20 dB gain Fabry-Perot cavity at 60 GHz were also proposed by Hosseini et al. [19].

This paper proposes a new hybrid approach where the stacking and superstrate schemes are extended in order to obtain an optimized antenna design that offers wide bandwidth and high gain. Our aim, from these investigations, is to reach a compromise between the two important antenna criteria: bandwidth and gain during the antenna design process. Our approach uses a dielectric resonator (DR), an aperture-coupled feed, a superstrate with some square ring FSS and a plain dielectric substrate, and an intermediate substrate. The starting antenna is an aperture coupled dielectric resonator antenna. The impedance bandwidth can be enhanced by merging the different resonant frequencies of the radiating slot and the DR. By adding an intermediate substrate, the structure will behave like a stacked DRA. Therefore, the gain will improve. Numerical results, taking into account the different physical parameters and operating conditions, are studied and compared to validate the design. Following this introduction, we present the proposed antennas in Section 2. Section 3 presents the validation of the design. Numerical data for the reflection coefficients, the gain, and the radiation pattern are shown. We proceed to verify, through simulations, the performance of the final antenna by using another software. Finally, the conclusion of this work is presented in Section 4.

## 2. Antenna Configuration

Figure 1 shows the geometry of the proposed wideband and high gain hybrid DRA. The proposed antenna is composed of a cylindrical dielectric resonator, an intermediate substrate, a superstrate with a periodic square ring FSS, and a microstrip fed slot. A microstrip line is printed on the other side of a grounded substrate. The line impedance of 50 Ω is designed with a strip width $W$. A stub of length $P$ is used to improve the impedance bandwidth. The thickness and the permittivity of the microstrip substrate are $\varepsilon_1$ and $h_1$, respectively. The coupling aperture, which is also a resonant one, is a narrow rectangular slot of length $L_s$ and width $W_s$. It is etched on a grounded substrate and it is located at the DRA center. The intermediate substrate of thickness $h_2$ and permittivity $\varepsilon_2$ is inserted between the dielectric resonator and the ground plane of the microstrip substrate. The intermediate substrate is a square of width $W_i$. The dielectric resonator antenna has a radius $R$, a height $H_{\text{dra}}$, and a dielectric constant $\varepsilon_{\text{dra}}$. A dielectric superstrate of permittivity $\varepsilon_{\text{sup}}$ is placed at a distance $d_s$ of the ground plane. This square superstrate has a $L_{\text{sup}}$, and a thickness $H_{\text{sup}}$. Furthermore, some square rings are placed in the lower side of the superstrate as shown in Figure 1(d). The unit cell of the square ring is depicted in Figure 1(e). Figure 1(c) shows the antenna with a plain dielectric as superstrate (antenna 3). Figures 1(a) and 1(b) illustrate a single DRA feed by a microstrip line through an aperture (antenna 1) without intermediate substrate, and with intermediate substrate (antenna 2), respectively.

## 3. FSS Modelling

CST microwave studio [20] was used to obtain the results for the unit cell of the square ring FSS. The reflection and transmission coefficients are obtained for a normal incident plane wave to the cell plane. CST uses some periodic boundary conditions in order to calculate the scattering parameters. The magnitude and the phase of the scattering parameters are shown on Figures 2 and 3, respectively. For the unit cell, the superstrate has a permittivity $\varepsilon_{\text{sup}} = 10.2$ and a thickness $H_{\text{sup}} = 0.4$ mm. The dimensions of the square ring are $S_o = 1.8$ mm and $S_i = 1.4$ mm. The distance $d_s$ can be deduced from the resonance condition as follows:

$$d_s = \frac{c}{2f}\left(\frac{\phi_{\text{PRS}} + \phi_{\text{Gnd}}}{2\pi}\right), \tag{1}$$

where $c$, $\phi_{\text{PRS}}$, $\phi_{\text{Gnd}}$, and $f$ are the velocity of light, the reflection phase of the FSS square ring, the reflection phase of the ground plane, and the operating frequency, respectively. At the frequency of 60 GHz, the value $\phi_{\text{PRS}}$ is 178°. The ground plane is a perfect electric conductor; therefore, $\phi_{\text{Gnd}}$ is equal to $\pi$. The value of $d_s$ is found to be $d_s = 2.4$ mm. The boresight gain relative to the feed antenna, which is a DRA in this case, is defined as [11]

$$G = \frac{1+R}{1-R}, \tag{2}$$

where $R$ is the reflection coefficient magnitude at the operating frequency. $R$ is found to be 0.89. The relative gain is 12.35 dBi. The DRA has a gain around 7 dBi; therefore, a FPC antenna of gain 19.35 dBi could be designed.

## 4. Design of the Antennas

CST microwave studio was also used to obtain the results for the transmission coefficient, return loss, and radiation patterns. For an aperture coupled scheme, only the $\text{TM}_{1np}$ modes of the Dielectric Resonator will be excited. The fundamental mode $\text{HEM}_{11\delta}$, also known as the $\text{TM}_{110}$, will be used. The electromagnetic behavior of this mode depends on the material properties of the DRA and its geometrical

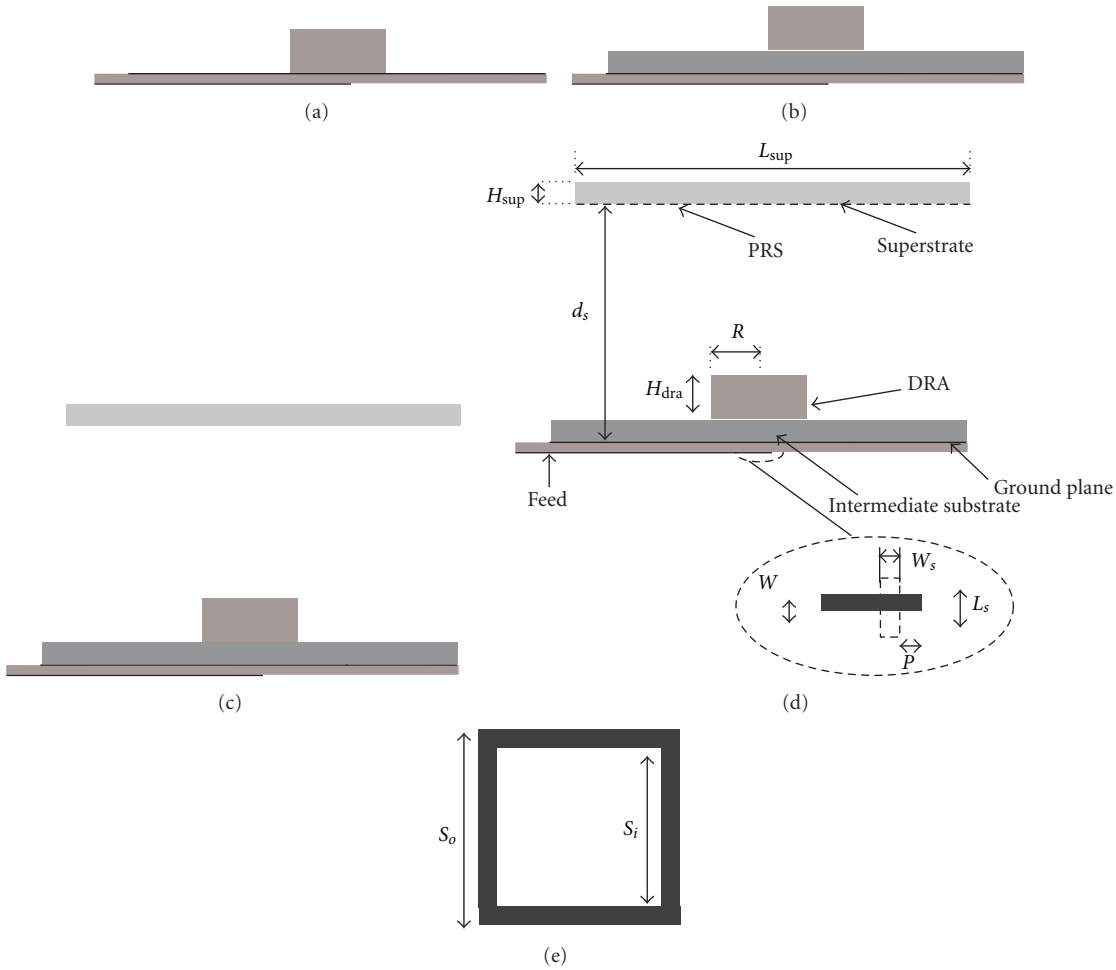


Figure 1: (a) Antenna 1, (b) antenna 2, (c) antenna 3, (d) FPC fed by a DRA, and (e) unit cell of the square ring FSS.

properties. The resonant frequency can be determined with the perfect magnetic conductor (PMC) wall approximation. The equation can be written as follows [4, 21]:

$$f_r = \frac{c}{2\pi\sqrt{\varepsilon_{\text{dra}}}}\sqrt{\left(\frac{1.841}{R}\right)^2 + \left(\frac{\pi}{2H_{\text{dra}}}\right)^2}, \tag{3}$$

where $c$ is the velocity of light, $H_{\text{dra}}$, $\varepsilon_{\text{dra}}$, and $R$ are the height, permittivity, and the radius of the dielectric resonator, respectively. 1.841 is the zero of derivative of the Bessel function $J_m = 0$. A resonant frequency of 49.24 GHz is obtained with $R_d = 1.5$ mm, $\varepsilon_{\text{dra}} = 10.2$, and $H_d = 0.5$ mm. The slot and the $\text{HEM}_{11\delta}$ mode of the cylindrical DRA radiate as horizontal magnetic dipoles. Therefore, a hybrid structure combining a slot and DRA can have multiresonant modes. If the different modes are correctly excited and near to each other and the closed multioperating frequency can be made to be less than −10 dB, a wide bandwidth response can be achieved.

Firstly, we designed the antenna with a single DRA feed by a microstrip line through an aperture. The structure has no intermediate substrate. This antenna is denoted antenna 1. The choice of the length of the aperture as well as the length of the open-ended microstrip line is important. The slot length will affect the coupling between the feed line and the DRA. The slot width is kept narrow for low cross-polarization. The slot is centered under the DRA. Its position is important to excite the correct mode for maximum coupling level. The microstrip has a permittivity $\varepsilon_1 = 2.2$ and a thickness $h_1 = 0.127$ mm, respectively. The antennas are fed by a microstrip line of width $W = 0.38$ mm to give a characteristic impedance of 50 Ω.

Figure 4 displays the reflection coefficient magnitude for antenna 1. This antenna has a bandwidth of 36.35% at the center frequency of 54.13 GHz. The slot length is $L_s = 1.3$ mm. The resonant frequency of the slot is around 60.12 GHz. The realized gain at broadside, which includes mismatch losses, is plotted in Figure 5. The simulated realized gain is around 6 dBi.

Secondly, the intermediate substrate of permittivity $\varepsilon_2 = 2.2$ and thickness $h_2 = 0.254$ mm is added to the previous structures. This is antenna 2. The resonant frequencies of the slot and of the DRA are expected to be dependent on the dimensions and the properties of the dielectric resonator and the intermediate substrate. The results of the reflection coefficient magnitude on Figure 4 show a bandwidth of 14.36%

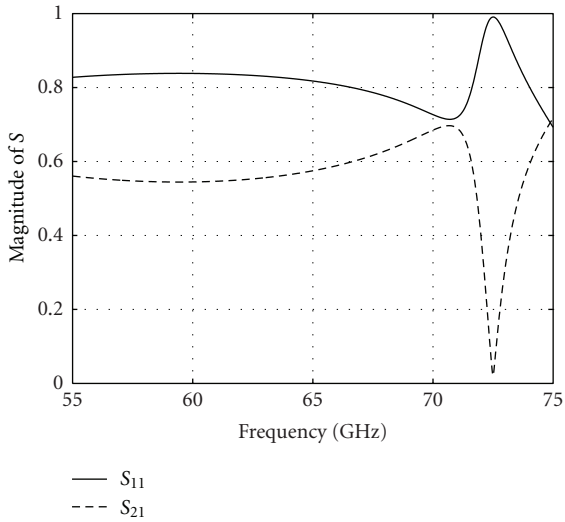


Figure 2: Magnitude of the transmission and reflection coefficients of the square ring FSS cell.

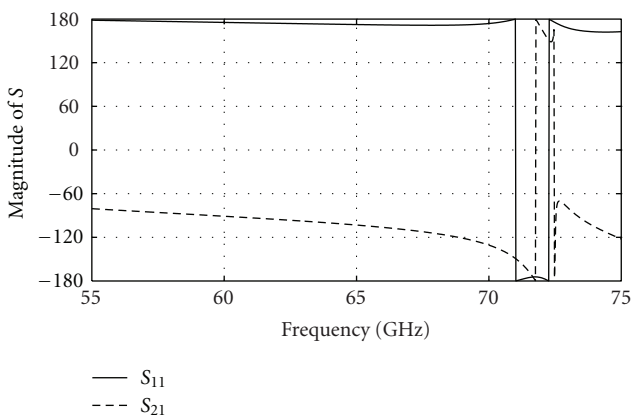


Figure 3: Phase of the transmission and reflection coefficients of the square ring FSS cell.

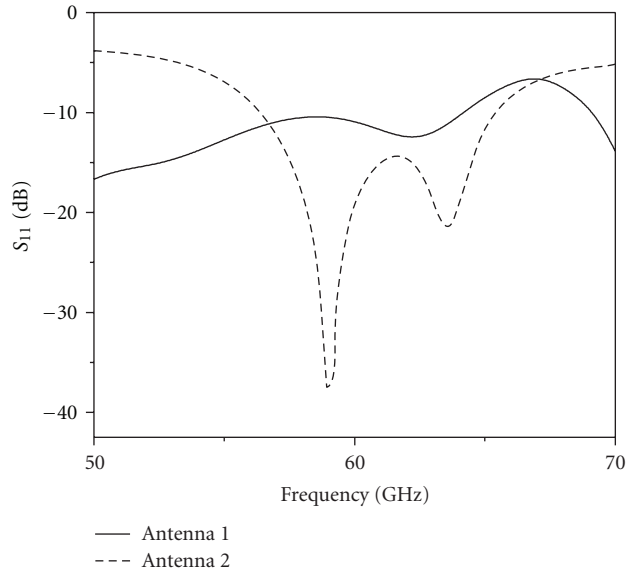


Figure 4: Reflection coefficient magnitude for antenna 1 and antenna 2.

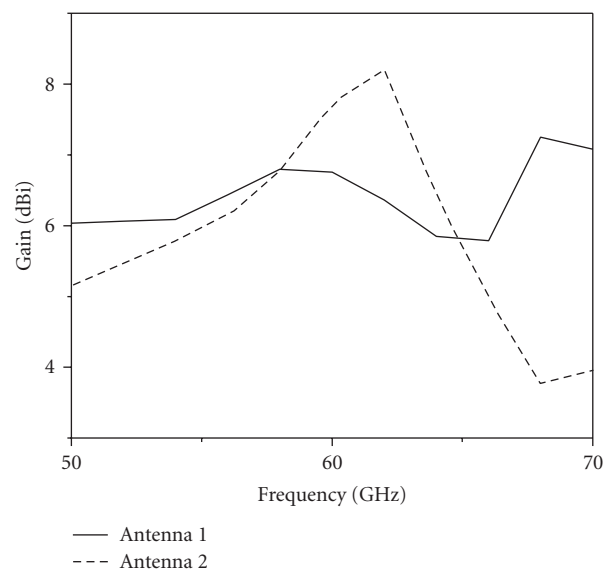


Figure 5: Realized gain for antenna 1 and antenna 2.

at the center frequency of 61.11 GHz. The gain, which is depicted in Figure 4, is around 6.8 dBi within the entire operating bandwidth. Clearly, the addition of the intermediate substrate increased the gain over the entire bandwidth.

Finally, the antennas with the square ring FSS and the plain dielectric superstrate are analyzed. These are antenna 3 and antenna 4. The superstrate has a permittivity $\varepsilon_{\text{sup}} = 10.2$ and a width $L_{\text{sup}} = 10$ mm. The FSS structure is made of four rows and four columns of the unit cell shown in Figure 1(b). The addition of the superstrate in the near field of the DRA will cause changes in the impedance bandwidth, the resonant frequencies, the gain, and the beam tilt. The superstrate can be placed over the DRA without having to redesign the DRA, but on the other hand a tuning of the impedance bandwidth must be done. Some antenna parameters have to be defined early on. The starting values of $d_{\text{sup}}$ and $H_{\text{sup}}$ are (2.4 mm) as obtained by (1) and $\lambda_g/4$ (0.4 mm), respectively. An intensive optimization was done. From Figure 6, it can be noted that antenna 3 and antenna 4 have an impedance bandwidth of 13.50% at the center frequency of 61.34 GHz and of 14.36% at the center frequency of 61.60 GHz, respectively. Figure 7 shows the realized gain of antenna 3 and antenna 4. For antenna 3, the peak realized gain is equal to 14.26 dBi. It is achieved at 60 GHz. The −3 dB radiation bandwidth is equal to 13.33%. For antenna 4, the optimum gain of 15.66 dBi is obtained at 60 GHz. Antenna 4 has 10% −3 dB radiation bandwidth. The gain is better than 11 dBi within the entire ISM frequency band for the two antennas. The best results of realized gain are achieved for $d_{\text{sup}} = 2.7$ mm and $d_{\text{sup}} = 2.8$ for antenna 3 and antenna 4, respectively. In all cases, $H_{\text{sup}}$ is not optimized, its value is $H_{\text{sup}} = 0.4$ mm.

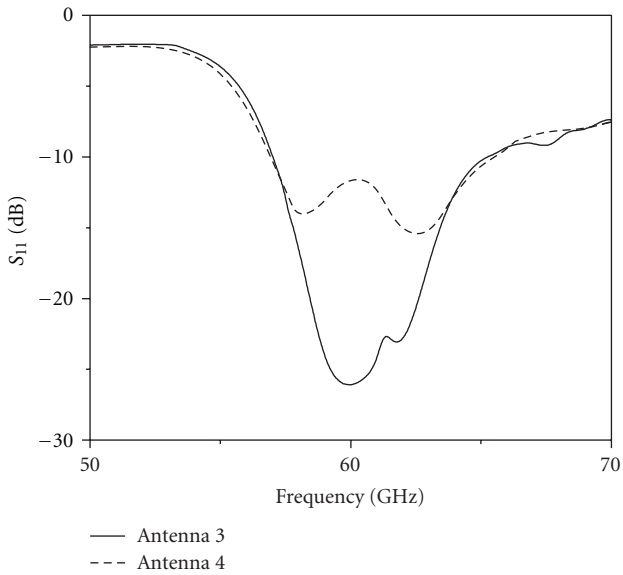


Figure 6: Reflection coefficient magnitude for antenna 3 and antenna 4.

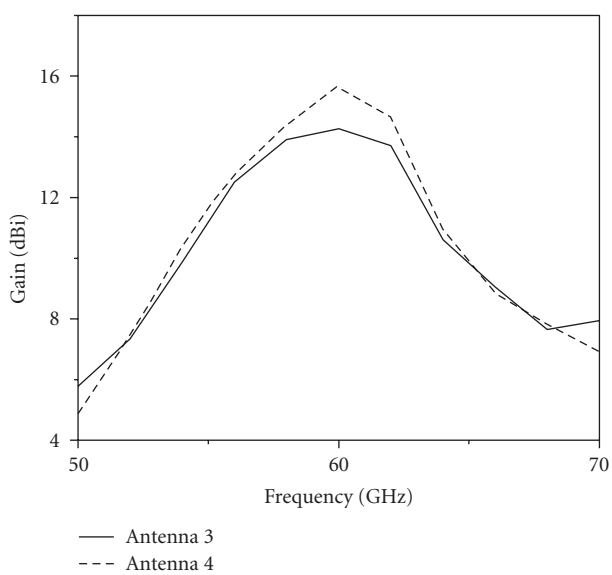


Figure 7: Realized gain for antenna 3 and antenna 4.

This kind of focusing system can be considered as an aperture antenna which can improve the effective aperture size of the DRA. The electric field distribution on the upper face of the superstrate is illustrated in Figure 8. The electric field varies on the superstrate. It is uniform in the center and decays at the edges. The superstrate will produce a high gain because it can be seen as an efficient aperture radiator with a large electrical area. Table 1 resumes all the other parameters of the four antennas.

Ansoft HFSS [22], another software package based on the finite method, is used as a tool to verify antenna characteristics. Both softwares use a waveguide port for their

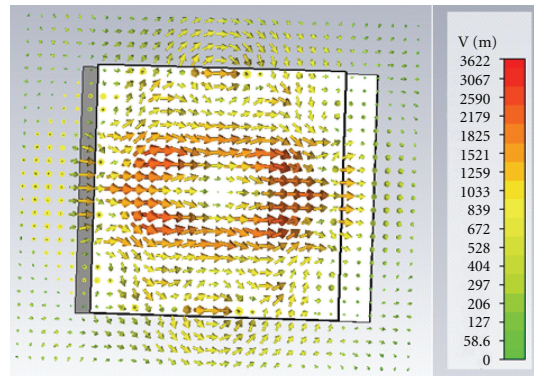


Figure 8: Electric-field distribution on the upper face of the superstrate at 60 GHz.

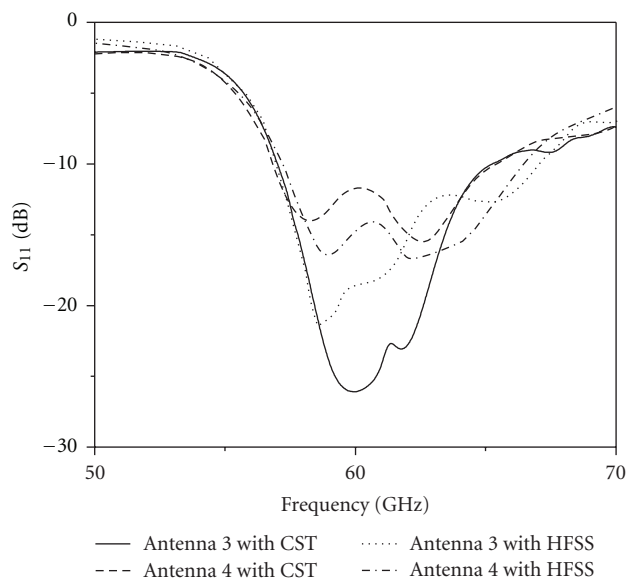


Figure 9: Comparison of the reflection coefficient magnitude for antenna 3 and antenna 4 with CST and Ansoft HFSS.

Table 1: Optimized parameters for antenna 1, antenna 2, antenna 3, and antenna 4.

| Parameters | Antenna 1 | Antenna 2 | Antenna 3 | Antenna 4 |
|---|---|---|---|---|
| $R_d$ (mm) | 1.50 | 1.50 | 1.50 | 1.50 |
| $P$ (mm) | 0.8 | 0.175 | 0.2 | 0.2 |
| $L_s$ (mm) | 1.2 | 1.5 | 1.5 | 1.65 |
| $W_s$ (mm) | 0.2 | 0.2 | 0.2 | 0.2 |

simulations. Figures 9 and 10 show the comparison of the impedance bandwidth and the gain with CST and Ansoft HFSS for antenna 3 and antenna 4. The resonant frequencies and the impedance bandwidth obtained from Figure 9 are reported in Table 2. It can be seen that there is an agreement between the results obtained by both softwares for antennas 3 and 4. There is a slight difference on the level of the return loss at both resonant frequencies and the two realized gains. The gain improvement is noted by the simulated results of

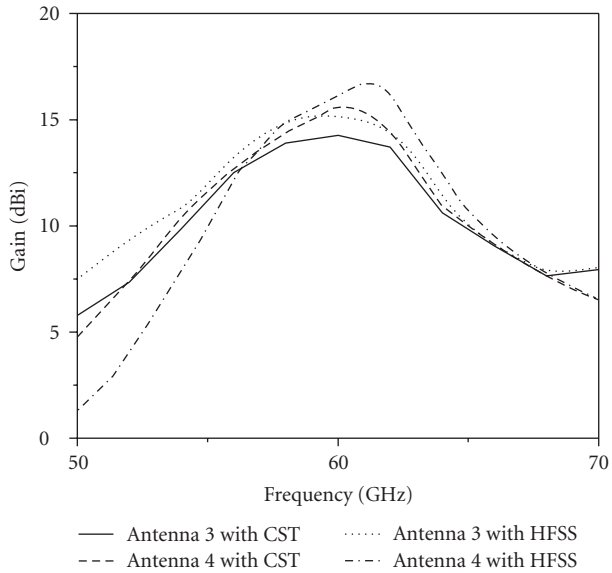


Figure 10: Comparison of the realized gain for antenna 3 and antenna 4 with CST and Ansoft HFSS.

Table 2: Comparisons of the results of antenna 5 and antenna 8 obtained with HFSS and CST.

| | Antenna 3 | Antenna 4 |
|---|---|---|
| $f_L$ using CST (GHz) | 59.98 | 58.20 |
| $f_L$ using HFSS (GHz) | 58.25 | 59 |
| $f_H$ using CST (GHz) | 61.9 | 62.68 |
| $f_H$ using HFSS (GHz) | 64 | 62.25 |
| Bandwidth using CST (%) | 13.50 | 14.36 |
| Bandwidth using HFSS (%) | 16.63 | 14.80 |

the two software packages. The difference can be explained by the fact that the two softwares used two different algorithm methods for the substrate losses at high frequencies, and meshing techniques.

The comparisons of the radiation patterns in the *E-plane* and *H-plane* at the operating frequency of 60 GHz, obtained with CST and Ansoft HFSS, for antenna 3 and antenna 4, are shown in Figure 11 and Figure 12, respectively. There is a good agreement between the radiation patterns obtained by the different softwares. The back radiation is reduced and the antenna beamwidth becomes narrow.

Table 3 compares the electromagnetic characteristics of the eight different antennas. Their performances are analyzed in terms of operating bandwidth, gain, 3 dB beamwidth in both planes, side lobe level in both planes, and angle of the main lobe in both planes. We can see that, by adding the intermediate substrate and the superstrate, the 3 dB beamwidth becomes narrower in both plane, and in the *E-plane* the main lobe tends to be in the broadside direction. In the *H-plane*, the main lobe is always in the broadside direction.

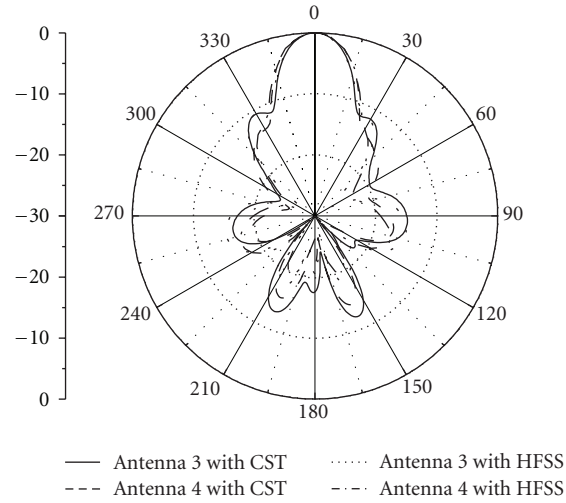


Figure 11: Comparisons of the copolarization radiation pattern at 60 GHz in the *E-plane* for the antenna 3 and antenna 4 with CST and Ansoft HFSS.

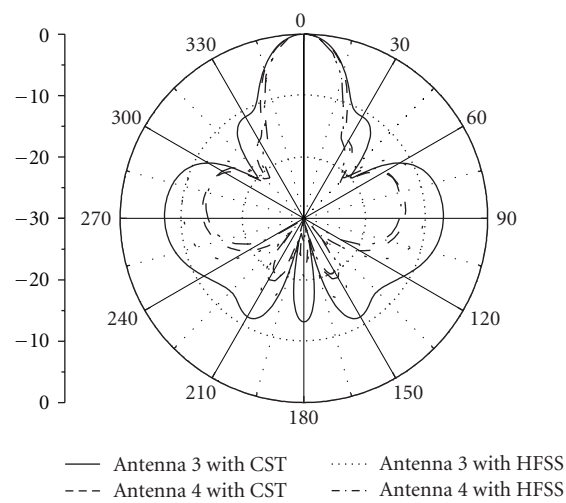


Figure 12: Copolarization radiation pattern at 60 GHz in the *H-plane* for antenna 1, antenna 2, antenna 3, and antenna 4.

## 5. Conclusion

An aperture-coupled scheme involving a superstrate and a hybrid Dielectric Resonator Antenna has been proposed in this paper. The gain was enhanced by adding a superstrate in order to cover the entire ISM band at 60 GHz and to recover the leaked energy due to the oxygen absorption at 60 GHz. By using a hybrid structure composed of a radiating slot and a DRA, the impedance bandwidth of the antenna was also increased. A bandwidth of 14.36% with reflection coefficient magnitude less than −10 dB at 61.60 GHz is obtained. The results showed that a gain enhancement of 10 dB was achieved at the frequency of 60 GHz. For one antenna, a maximum gain of 15.56 dB was reached, and for all antennas the gain was better than 11 dB within the ISM

Table 3: Comparison of the characteristics of the proposed antennas.

| Antennas | 1 | 2 | 3 | 4 |
|---|---|---|---|---|
| Bandwidth (%) | 36.5 | 14.36 | 13.50 | 14.36 |
| Gain at 60 GHz dBi | 6.9 | 7.8 | 14.36 | 15.7 |
| 3 dB beamwidth *E-plane* (°) | 142.3 | 69.6 | 20.7 | 22.9 |
| 3 dB beamwidth *H-plane* (°) | 51 | 73.1 | 23.9 | 23.1 |
| Angle of main lobe *E-plane* (°) | 50 | 3 | 0 | 0 |
| Angle of main lobe *H-plane* (°) | 0 | 0 | 0 | 0 |
| Side lobe level *E-plane* dB | −8.9 | −8.4 | −10.7 | −14.3 |
| Side lobe level in *H-plane* dB | −16.3 | −14.1 | −9.7 | −13.3 |

frequency bandwidth (57 GHz–64 GHz). Two different softwares are used to validate the optimized designs. With the obtained results, these antennas can be suitable for underground wireless communications systems.

## Acknowledgment

The authors gratefully acknowledge support for this research from the National Science Engineering Research Council of Canada (NSERC).

## References

[1] S. Outalha, R. Le, and P.-M. Tardif, "Toward a unified and digital communication system for underground mines," *CIM Bulletin*, vol. 93, no. 1044, pp. 100–105, 2000.

[2] P. F. M. Smulders, "60 GHz radio: prospects and future directions," in *Proceedings of the IEEE Symposium Benelux Chapter on Communications and Vehicular Technology*, pp. 1–8, Eindhoven, The Netherlands, 2003.

[3] M. Nedil, A. M. Habib, A. Djaiz, and T. A. Denidni, "Design of new mm-Wave Antenna fed by CPW Inductively Coupling fo mining communication," *IEEE Antenna and Propagation Society*, pp. 1–4, 2009.

[4] K. M. Luk and K. W. Leung, *Dielectric Resonators Antennas*, Research Studies Press, Hertfordshire, UK, 2002.

[5] Y. Hwang, Y. P. Zhang, K. M. Luk, and E. K. N. Yung, "Gain-enhanced miniaturised rectangular dielectric resonator antenna," *Electronics Letters*, vol. 33, no. 5, pp. 350–352, 1997.

[6] Nasimuddin and K. P. Esselle, "A low-profile compact microwave antenna with high gain and wide bandwidth," *IEEE Transactions on Antennas and Propagation*, vol. 55, no. 6, pp. 1880–1883, 2007.

[7] T. A. Denidni, Y. Coulibaly, and H. Boutayeb, "Hybrid Dielectric resonator with circular Musroom-like Stucture for gain improvement," *IEEE Transactions on Antennas and Propagation*, vol. 57, no. 4, pp. 1043–1049, 2009.

[8] A. A. Kishk, B. Ahn, and D. Kajfez, "Broadband stacked dielectric resonator antennas," *Electronics Letters*, vol. 25, no. 18, pp. 1232–1233, 1989.

[9] A. A. Kishk, Y. Yin, and A. W. Glisson, "Conical dielectric resonator antennas for wide-band applications," *IEEE Transactions on Antennas and Propagation*, vol. 50, no. 4, pp. 469–474, 2002.

[10] A. Buerkle, K. Sarabandi, and H. Mosallaei, "Compact slot and dielectric resonator antenna with dual-resonance, broadband characteristics," *IEEE Transactions on Antennas and Propagation*, vol. 53, no. 3, pp. 1020–1027, 2005.

[11] A. P. Feresidis and J. C. Vardaxoglou, "High gain planar antenna using optimised partially reflective surfaces," *IEE Proceedings*, vol. 148, no. 6, pp. 345–350, 2001.

[12] J. Ju, D. Kim, W. J. Lee, and J. I. Choi, "Wideband high-gain antenna using metamaterial superstrate with the zero refractive index," *Microwave and Optical Technology Letters*, vol. 51, no. 8, pp. 1973–1976, 2009.

[13] A. Foroozesh and L. Shafai, "Investigation into the effects of the patch-type FSS superstrate on the high-gain cavity resonance antenna design," *IEEE Transactions on Antennas and Propagation*, vol. 58, no. 2, pp. 258–270, 2010.

[14] R. Chantalat, L. Moustafa, M. Thevenot, T. Monediere, and B. Jecko, "Low profile EBG resonator antennas," *International Journal of Antennas and Propagation*, vol. 2009, Article ID 394801, 7 pages, 2009.

[15] X. H. Wu, A. A. Kishk, and A. W. Glisson, "A transmission line method to compute the far-field radiation of arbitrary Hertzian dipoles in a multilayer structure embedded with PEC strip interfaces," *IEEE Transactions on Antennas and Propagation*, vol. 55, no. 11 II, pp. 3191–3198, 2007.

[16] R. Mittra, Y. Li, and K. Yoo, "A comparative study of directivity enhancement of microstrip patch antennas with using three different superstrates," *Microwave and Optical Technology Letters*, vol. 52, no. 2, pp. 327–331, 2010.

[17] S. J. Franson and R. W. Ziolkowski, "Gigabit per second data transfer in high-gain metamaterial structures at 60 GHz," *IEEE Transactions on Antennas and Propagation*, vol. 57, no. 10, pp. 2913–2925, 2009.

[18] H. Vettikalladi, O. Lafond, and M. Himdi, "High-efficient and high-gain superstrate antenna for 60-GHz indoor communication," *IEEE Antennas and Wireless Propagation Letters*, vol. 8, pp. 1422–1425, 2009.

[19] S. A. Hosseini, F. Capolino, and F. De Flaviis, "Design of a single-feed 60 GHz planar metallic Fabry-Perot cavity antenna with 20 dB gain," in *Proceedings of the IEEE International Workshop on Antenna Technology (iWAT '09)*, Santa Monica, Calif, USA, March 2009.

[20] CST Microwave Studio, v. 2011.

[21] S. A. Long, M. W. McAllister, and L. C. Shen, "The resonant cylindrical dielectric cavity antenna," *IEEE Transactions on Antennas and Propagation*, vol. 31, no. 3, pp. 406–412, 1983.

[22] Ansoft HFSS, v. 12.